High-resolution photoemission study of the interaction of hydrogen with GaAs(110) surfaces

L. Sorba,* M. Pedio,† and S. Nannarone
Dipartimento di Fisica dell'Università di Roma "La Sapienza," piazzale Aldo Moro 2, I-00185 Roma, Italy

S. Chang,‡ A. Raisanen, A. Wall,§ P. Philip, and A. Franciosi
Department of Chemical Engineering and Materials Science, University of Minnesota, Minneapolis, Minnesota 55455
(Received 13 June 1988; revised manuscript received 13 June 1989)

We present a synchrotron-radiation photoemission investigation of hydrogen chemisorption on GaAs(110) surfaces cleaved *in situ*. Analysis of the valence-band emission and high-resolution core photoemission studies as a function of hydrogen coverage and photoelectron escape depth show that at least in the high-coverage regime hydrogen chemisorption occurs *via* the formation of surface bonds between atomic hydrogen and both As and Ga atoms. Decomposition of the As 3*d* and Ga 3*d* core lines in terms of bulk and surface components demonstrates that hydrogen adsorption is accompanied by preferential etching of As, roughening of the surface, and a consequent relatively large variation of surface stoichiometry toward a Ga-rich composition.

I. INTRODUCTION

Hydrogen chemisorption on GaAs surfaces constitutes one of the simplest model systems to study the effect of chemisorption on surface atomic and electronic structure in compound semiconductors.[1–15] A strong technological motivation derives from the importance of hydrogen-ion etching and hydrogen incorporation during processing of III-V semiconductor materials. The kinetics of hydrogen diffusion, the bonding of hydrogen in the semiconductor matrix and, conversely, the effect of hydrogen on the local structure of the host, are still subjects of intense debate.[1–18]

The interaction of hydrogen with the nonpolar (110) surfaces of GaAs has been recently studied with temperature-programmed desorption,[6] ultraviolet photoemission spectroscopy (UPS),[9] electron-energy-loss[11] (ELS) and Auger[11] spectroscopy. Most results suggest a chemisorption process qualitatively different at low versus high hydrogen coverages, where "high" coverages are defined as coverages near or at saturation (~ 1 monolayer). For example, Sebenne and co-workers[11] reported no observable change in Ga- or As-related Auger lines at low hydrogen exposure, but observed a substantial decrease in the intensity of both Auger features near saturation. They interpreted this as evidence that hydrogen chemisorbs on both Ga and As atoms at high coverage. In contrast with this, core photoemission studies of hydrogen chemisorption on GaAs(100) and GaAs($\bar{1}\,\bar{1}\,\bar{1}$) polar surfaces by Bringans and Bachrach,[4] showed no effect on the Ga 3*d* line shape. The As 3*d* core emission showed[4] hydrogen-induced high-binding-energy components. Bringans and Bachrach concluded that hydrogen is mainly bonded to As atoms on both (100) and ($\bar{1}\,\bar{1}\,\bar{1}$) surfaces.

Chemisorption of hydrogen on GaAs surfaces has been shown to yield changes in surface stoichiometry, but direction, magnitude, and interpretation of the changes are still controversial. Bartels *et al.*[5] reported a 20% increase in the $I(\mathrm{Ga})/I(\mathrm{As})$ Auger intensity ratio after exposure to about 3×10^4L of hydrogen for GaAs(110), and interpreted this as evidence of As loss. Sebenne and co-workers[11] reported a similar 15% increase in the $I(\mathrm{Ga})/I(\mathrm{As})$ Auger ratio on GaAs(110), but associated the change with a modification in surface reconstruction that makes the Ga atoms "more visible" without preferential desorption of As. At higher coverage they associated further increase in the $I(\mathrm{Ga})/I(\mathrm{As})$ Auger intensity ratio to dissociation of the surface in metallic Ga droplets and AsH_3. The latter would remain chemisorbed on the surface[11] without contributing to the Auger signal because of the rearrangement of the As orbitals involved in the Auger process.[11] Chemisorption of atomic hydrogen on GaAs(110) at 250 K followed by temperature-programmed desorption[6] showed that, at least in the high-coverage case, desorption of hydrogen in molecular form is preceded by desorption of AsH_3 at room temperature (starting at 280 K), yielding presumably a Ga-rich surface.

In photoemission experiments focusing on Ga- and As-rich GaAs(100) and GaAs($\bar{1}\,\bar{1}\,\bar{1}$) surface reconstructions, Bringans and Bachrach[4] observed change in surface stoichiometry upon hydrogen adsorption, with convergence to a single As-rich final stoichiometry of the H-covered surface. Sublimation of gallium hydrides or As diffusion to the surface were proposed to explain the change in composition of initially Ga-rich surfaces.[4]

The apparent discrepancy between the photoemission results of Ref. 4 and the Auger results of Refs. 5 and 11 might be related, at least in part, to the different surface orientations employed. To our knowledge, no high-resolution photoemission results are available for GaAs(110)-H to be compared with the Auger[5] and temperature-programmed desorption[6] studies on the same surface. We report here soft-x-ray high-resolution photoemission studies of the Ga and As core emission from the GaAs(110) surface as a function of hydrogen exposure and photoelectron escape depth, complemented

by UPS studies of the hydrogen-induced modification of the valence states. Our high-resolution measurements allowed us to analyze the As and Ga core line shapes in terms of bulk and surface-related contributions, and follow the modification of the surface potential and surface composition as a function of hydrogen coverage. We focus here on the high-hydrogen-coverage regime and provide evidence of direct bonding of atomic hydrogen to Ga and As surface atoms. We discuss the corresponding bond ionicity, and quantify the variation in surface composition that results from hydrogen-induced preferential desorption of As.

II. EXPERIMENT

The experiments were conducted on oriented GaAs single crystals, Te doped, with resistivity of 10 Ω cm. Crystals $4\times4\times10$ mm^3 in size were cleaved in a photoelectron spectrometer at an operating pressure $<5\times10^{-11}$ Torr. Hydrogen exposures were performed isolating the ion pumps from the spectrometer, but with a liquid-nitrogen-cooled cryopanel in operation to reduce the background pressure and eliminate water.[11] Atomic hydrogen was obtained with a hot tungsten filament (2200 K) not in line of sight of the sample surface at a molecular hydrogen pressure of 10^{-5} Torr. The molecular pressure was monitored with a low-emission ion gauge, and in what follows exposures will be given in langmuirs in terms of the measured molecular pressure, since no direct measurement of the atomic hydrogen flux was performed. Such "nominal" exposures can be converted in actual hydrogen coverage of the surface by monitoring with ELS the intensity of the GaAs surface exciton as a function of hydrogen exposure.[7,12] We measured a coverage of approximately 1 monolayer at 5250 L hydrogen exposure. Therefore all of the data discussed in the present work pertain to the high-coverage saturation regime.

After exposure to hydrogen the samples were positioned at the focus of a monochromatic synchrotron-radiation beam and an electron analyzer. Radiation emitted by the electron storage ring Aladdin at the Synchrotron Radiation Center of the University of Wisconsin–Madison, or by the Adone facility in Frascati, Italy, was monochromatized (in both cases) with a grazing incidence "grasshopper" monochromator. We used a commercial hemispherical analyzer or a double-pass cylindrical mirror analyzer to record angular-integrated photoelectron energy distribution curves (EDC's) in the $40<h\nu<140$ eV photon energy range. The experimental energy resolution and Fermi-level position were measured from the width and position of the Fermi cutoff in EDC's from metal films evaporated *in situ*.[19] Overall resolution was 0.18 eV at $h\nu=40$ eV, 0.15 eV at $h\nu=70$ eV, and 0.22 eV at $h\nu=100$ eV. The monochromator throughput was monitored through the total yield of a Ni or Al mesh positioned at the exit slit of the monochromator.

Representative EDC's for the Ga 3*d*, As 3*d*, and valence-band emission as a function of hydrogen coverage are shown in Figs. 1–4 after subtraction of a smooth secondary electron background estimated with a polynomial fit of the high- and low-energy spectral range.

III. RESULTS AND DISCUSSION

A. Core-level decomposition

In Fig. 1 we show the Ga 3*d* core emission as a function of hydrogen exposure at a photon energy of 80 eV. The experimental spectra (solid circles) are given in relative units after normalization to monochromator throughput, and are shown superimposed to the result of a fit (solid line) in terms of up to three Ga 3*d*-derived doublets. The zero of the binding energy scale is referred to the position of the $3d_{5/2}$ component that corresponds to the bulk core emission, so that the binding-energy values are implicitly corrected for variations in band bending. The topmost EDC in Fig. 1 corresponds to the clean GaAs(110) emission, while spectra displaced downward show the effect of increasing hydrogen exposure. Upon exposure, the EDC's in Fig. 1 show the emergence of a high-binding-energy component that causes a markedly asymmetric broadening of the experimental line. A similar feature is observed at photon energies of 60 and 70 eV, albeit with a reduced intensity, due to a reduction in surface sensitivity.[20–23]

The different Ga 3*d* spin-split components were approximated with Lorentzian functions convoluted with a Gaussian function. The clean GaAs(110) Ga 3*d* spectra were decomposed in terms of a bulk spin-split 3*d* doublet and a surface-related doublet. Peak position, intensity, branching ratio, spin-orbit splitting, full width at half maximum (FWHM) of the Gaussian functions and half width at half maximum (HWHM) of the Lorentzian functions were treated at fitting parameters. The secondary electron background was introduced as a third-order polynomial, with coefficients treated also as fitting parameters. A least-squares minimization yielded the line-shape parameters shown in the first rows of Tables I and II, at photon energies of 80 and 60 eV, respectively. The quality of the fit was monitored through the average deviation of the experimental data from the theoretical curve, and is given as a percentage of the experimental peak intensity [average percent variation APV]. The values of the parameters for the clean surface core emission are consistent, within experimental uncertainty, with those obtained by Eastman and Himpsel,[21] and Ludeke *et al.*[24] We find, for example, a surface Ga 3*d* doublet shifted 0.28 ± 0.02 eV (Ref. 25) to higher binding energy relative to the main bulk line (0.28 eV in Ref. 22), and a spin-orbit splitting of 0.44 eV (0.45 eV in Ref. 24). We also note that the Gaussian FWHM in Tables I and II are consistent with the measured experimental energy resolution,[19] and that the Lorentzian HWHM Γ remain invariant with photon energy.[23] All of these observations support the validity of the fitting procedure employed.

Surface shifts in core-level binding energies have been observed in a number of III-V (Refs. 20–22) and II-VI semiconductors.[27] Recently Monch has argued[20] that the core-level shifts observed in III-V semiconductors can be explained solely in terms of the reduction of the

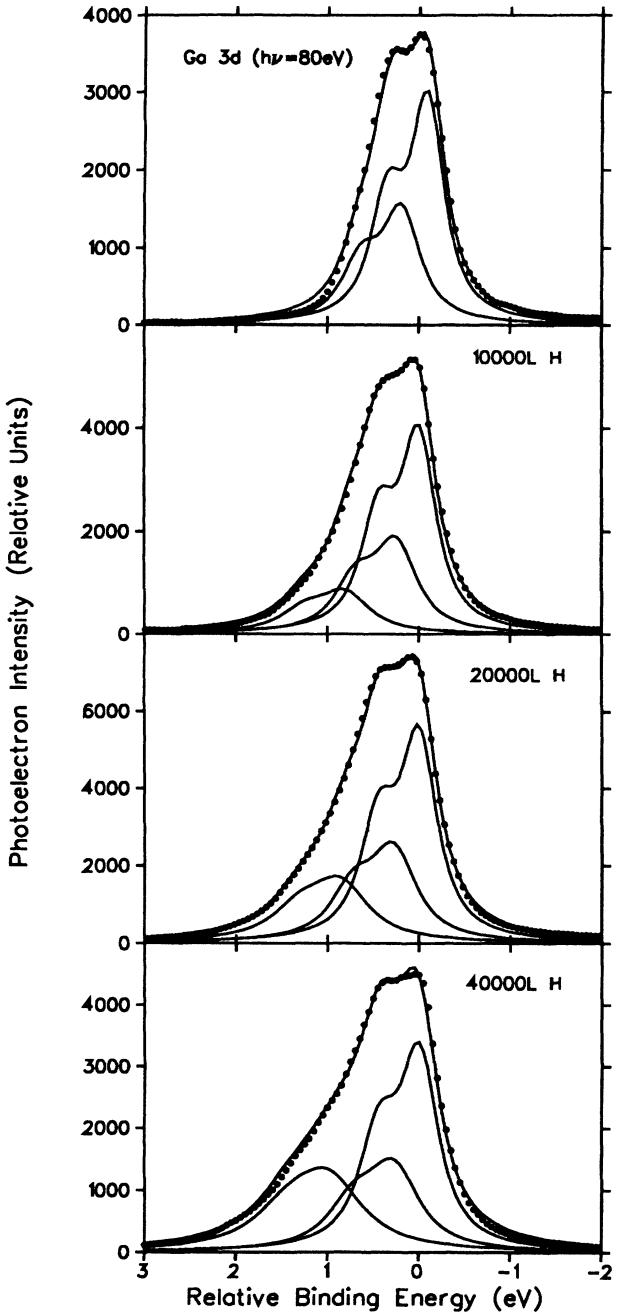

FIG. 1. High-resolution photoelectron energy distribution curves (EDC's) at $h\nu=80$ eV for the Ga $3d$ core emission from GaAs(110) at increasing atomic hydrogen exposure. The nominal exposure in langmuirs is calculated in terms of the molecular hydrogen pressure in the system. A hot tungsten filament was used to dissociate hydrogen near the sample surface. The solid circles are experimental points, and appear superimposed to the result of a least-squares fit (solid line) of the EDC's in terms of up to three individual Ga $3d$ doublets. Each doublet included two spin-split Lorentzian lines convoluted with a Gaussian function. The resulting individual doublets, reflecting the bulk (rightmost doublet), surface-related (center), and hydrogen-induced (leftmost doublet) Ga $3d$ emission are also shown (solid line). The experimental EDC's are normalized to the monochromator throughput and are given in relative units. The 0 of the binding-energy scale corresponds to the position of the bulk Ga $3d_{5/2}$ level.

Madelung potential near the surface,[28] which should make the surface less ionic. However, Prince *et al.*[27] have proposed that the surface core-level shifts observed in CdTe are quantitatively not consistent with such a model, and suggested that rehybridization (i.e., changes in covalent bonding) at the surface may oppose the trend toward lower surface ionicity, as pointed out earlier by Watson and Devenport.[29] The existence of such surface shifts allows us to single out the effect of chemisorption on the surface atoms, and obtain quantitative information on the resulting surface modification.

Upon exposure to hydrogen in Fig. 1, two Ga $3d$ doublets cannot reproduce the experimental line for any reasonable choice of parameters, so that three doublets were employed. Peak positions, intensities, and widths of the Lorentzian and Gaussian functions were treated as fitting parameters. The spin-orbit splitting and branching ratio were fixed at the values obtained from the bulk and surface-shifted doublets prior to hydrogen exposure. The three different doublets resulting from the fitting procedure are shown (solid line) in Fig. 1. In Tables I and II we give the value of the relevant fitting parameters as obtained from the Ga $3d$ least-squares fitting procedure at photon energies of 80 and 60 eV, respectively.

With increasing hydrogen exposure in Fig. 1 we observe a reduction in the relative intensities of Ga $3d$ bulk and surface components, and the emergence of a new high-binding-energy doublet some 0.80 eV (10^4 L) below the bulk component. We associate this new component with the reaction of Ga surface atoms with atomic hydrogen. The binding energy E_h of the hydrogen-induced feature increases slightly with hydrogen exposure, and is found 0.98 ± 0.05 eV (Ref. 25) below the bulk Ga $3d$ emission (at all photon energies) at the maximum exposures explored. The increase in the Ga chemical shift from 0.80 to 0.98 eV, and the corresponding increase in Lorentzian width from 0.30 to 0.42 eV, may be due to the emergence of unresolved high-binding-energy components, as will be explained in Sec. III C.

The overall intensity of the hydrogen-induced plus surface-related Ga $3d$ emission increases dramatically with hydrogen exposure, but appears to saturate at the highest coverages explored. The hydrogen-induced broadening of the individual Ga $3d$ doublets observed in Fig. 1 derives mostly from an increase in Lorentzian rather than Gaussian broadening. The Lorentzian HWHM for the surface and hydrogen-induced doublets in Table I increase from 0.22 and 0.30 eV to 0.30 and 0.42 eV, respectively, with hydrogen exposure, while the Gaussian widths remain relatively constant. We explored a number of different methods for background subtraction and line-shape analysis, with consistent results. For example, we present in the two bottom-most rows of Table I lineshape parameters obtained through a fitting procedure in which the Lorentzian and Gaussian widths, respectively, of the surface and hydrogen-related Ga $3d$ levels (at 4×10^4 L exposure) were kept fixed at the initial values. We note that while fixing the Gaussian widths has relatively little effect on the APV parameter, fixing the Lorentzian widths yields a large increase in the APV parameter. This is not an artifact of the background sub-

TABLE I. Ga 3*d* line-shape parameters obtained from a least-squares fit of the EDC's of Fig. 1 at $h\nu=80$ eV in terms of the superposition of surface, bulk, and hydrogen-induced Ga 3*d* doublets. Each doublet included two spin-split Lorentzian lines convoluted with a Gaussian function. Spin-orbit splitting and branching ratio of the doublets were kept fixed at the value determined from the clean surface results (0.44 and 0.57 eV, respectively). Binding energies (in eV) are referred to the bulk Ga $3d_{5/2}$ binding energy. Column 1: hydrogen exposure in langmuirs. Column 2: average percent variation of the experimental points relative to the theoretical line shape, expressed as percent of the experimental peak amplitude. Columns 3 and 4: binding energy of the surface (E_s) and hydrogen-induced (E_h) $3d_{5/2}$ components. Columns 5 and 6: Lorentzian half widths at half maximum (HWHM) Γ_b and Gaussian full width at half maximum (FWHM) Δ_b in eV for the Ga 3*d* bulk subcomponents. Columns 6, 7, 8, 9, and 10: HWHM Γ and a FWHM Δ for the surface (subscript *s*) and hydrogen-induced (subscript *h*) subcomponents. Column 11: integrated intensity of the surface Ga 3*d* doublet relative to the bulk-related 3*d* doublet. Column 12: intensity of the hydrogen-induced doublet relative to the surface doublet. Column 13: integrated intensity of the overall surface (surface + hydrogen-induced) 3*d* emission relative to the bulk 3*d* emission. In the fifth and sixth rows of the table we show line-shape parameters obtained keeping Lorentzian HWHM and Gaussian FWHM, respectively, fixed at the initial values.

		Ga 3*d* ($h\nu=80$ eV)										
	APV	E_s	E_h	Γ_b	Δ_b	Γ_s	Δ_s	Γ_h	Δ_h	I_s/I_b	I_h/I_s	$(I_s+I_h)/I_b$
clean	1.0%	0.28		0.19	0.16	0.22	0.16			0.55	0.00	0.55
1×10^4 L	1.0%	0.27	0.80	0.21	0.16	0.24	0.17	0.30	0.16	0.54	0.52	0.82
2×10^4 L	0.7%	0.27	0.86	0.21	0.16	0.27	0.17	0.35	0.17	0.55	0.78	0.98
4×10^4 L	1.2%	0.27	0.98	0.23	0.16	0.30	0.18	0.42	0.17	0.54	1.11	1.15
					Fixed Lorentzian widths							
4×10^4 L	2.2%	0.27	0.99	0.19	0.16	0.22	0.17	0.22	0.17	0.54	0.99	1.08
					Fixed Gaussian widths							
4×10^4 L	1.3%	0.27	0.98	0.23	0.16	0.30	0.16	0.42	0.16	0.49	1.14	1.04

TABLE II. Ga 3*d* line-shape parameters obtained from a least-squares fitting procedure of the EDC's for the Ga 3*d* emission at $h\nu=60$ eV. The procedure and the symbols employed are identical to those used in Table I. Note the lower surface sensitivity of the results at $h\nu=60$ eV as compared to the results at $h\nu=80$ eV.

		Ga 3*d* ($h\nu=60$ eV)										
	APV	E_s	E_h	Γ_b	Δ_b	Γ_s	Δ_s	Γ_h	Δ_h	I_s/I_b	I_h/I_s	$(I_s+I_h)/I_b$
clean	1.7%	0.28		0.19	0.13	0.19	0.12			0.49	0.00	0.49
1×10^4 L	1.5%	0.28	0.78	0.20	0.15	0.25	0.15	0.30	0.15	0.49	0.41	0.69
2×10^4 L	1.5%	0.27	0.83	0.20	0.15	0.27	0.15	0.35	0.15	0.54	0.67	0.90
4×10^4 L	1.4%	0.26	0.99	0.23	0.15	0.30	0.15	0.43	0.15	0.52	0.98	1.02

traction procedure, which could in principle affect the determination of the Lorentzian low-binding-energy tail, since the background parameters were also treated as fitting parameters. We associate the increase in Lorentzian width with an asymmetric broadening of the Ga 3*d* line due to the formation of disordered, Ga-rich surface and near-surface layers. This point will be further discussed in Sec. III C. We emphasize that whichever method one may want to employ for the fit, binding energies and relative intensities of the Ga 3*d* bulk, surface, and hydrogen-induced components remain largely unchanged (see, for example, the corresponding values in the three bottom-most rows of Table I).

An analysis similar to that described for the Ga 3*d* core levels was performed for the As 3*d* levels. Experimental EDC's (solid circles) together with the results of a least-squares fitting procedure are shown in Fig. 2 at a photon energy of 100 eV. Results at a photon energy of $h\nu=80$ eV are qualitatively similar except for a reduced surface sensitivity.[20,30] Prior to hydrogen exposure the EDC's could be decomposed in terms of a bulk 3*d* doublet and a surface-related doublet. The corresponding fitting parameters are shown in the first row of Tables III and IV. As in the case of the Ga 3*d* emission, all of the resulting parameters were consistent, within experimental uncertainty, with the results of Refs. 22 and 24. For example, we found a surface shift of 0.39 ± 0.03 eV to lower binding energy for the As 3*d* line (0.37 eV in Ref. 22), a spin-orbit splitting of 0.70 ± 0.03 eV (0.70 eV in Ref. 22), and a branching ratio of 0.62 (0.65 ± 0.05 in Ref. 24).[25]

Upon hydrogen exposure, superposition of three As 3*d* doublets was required to reproduce the experimental EDC's. We fixed the As 3*d* spin-orbit splitting and branching ratio to the value obtained from the EDC's for the clean surface emission, and determined binding energies, relative intensities, Gaussian and Lorentzian widths, and the background through a least-squares fitting procedure. Representative fitting parameters are shown in Tables III and IV for photon energies of 100 and 80 eV, respectively. The quality of the fits is somewhat lower than that obtained for the Ga 3*d* core levels in Tables I and II, but the average percent deviation is at most 1.7% of the experimental peak amplitude.

The least-squares analysis shows that the broadening of the experimental EDC's in Fig. 2 corresponds to a decrease in the emission from the surface doublet, together with the emergence of an hydrogen-induced As 3*d* doublet 0.30 ± 0.05 eV below the position of the bulk As 3*d* doublet. We associate this contribution with the formation of chemical bonds between As surface atoms and atomic hydrogen.

The binding energies of the individual As 3*d* doublets remain consistent as a function of photon energy within an experimental uncertainty of ±0.05 eV, and this supports the validity of the fitting procedure employed. With hydrogen exposure we observe a limited increase in the Lorentzian width of the surface-related doublet in Tables III and IV, while the Gaussian widths remain relatively constant. As for the Ga 3*d* emission, we have explored different fitting procedures, with consistent results. For example, we present in the fifth and sixth rows of

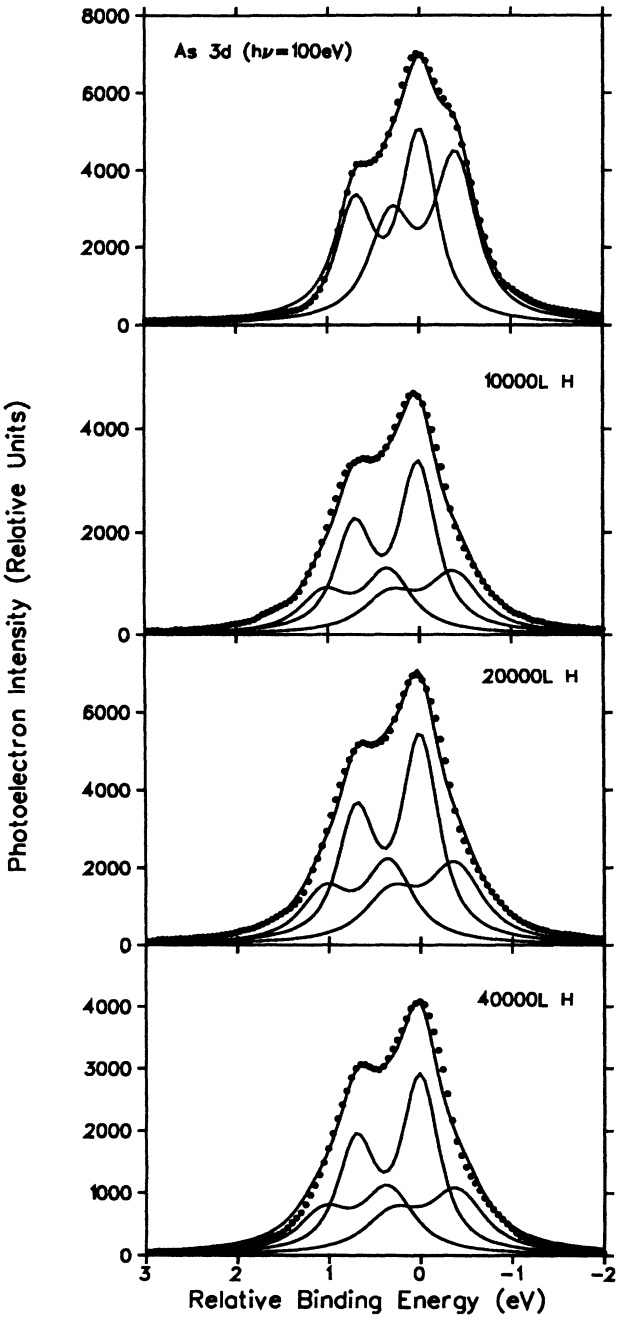

FIG. 2. High-resolution EDC's at $h\nu=100$ eV for the As 3*d* core emission from GaAs(110) at increasing atomic hydrogen exposure. The solid circles are experimental points, and appear superimposed to the result of a least-squares fit (solid line) of the EDC's in terms of up to three individual Ga 3*d* doublets. Each doublet included two spin-split Lorentzian lines convoluted with a Gaussian function. The resulting individual doublets, reflecting the bulk (center), surface-related (rightmost doublet), and hydrogen-induced (leftmost doublet) As 3*d* emission are also shown (solid line). The experimental EDC's are normalized to the monochromator throughput and are given in relative units. The zero of the binding-energy scale corresponds to the position of the bulk As $3d_{5/2}$ level.

TABLE III. As 3*d* line-shape parameters obtained from a least-squares fit of the EDC's of Fig. 2 in terms of the superposition of surface, bulk, and hydrogen-induced As 3*d* doublets. Each doublet included two spin-split Lorentzian lines convoluted with a Gaussian function. Spin-orbit splitting and branching ratio of the doublets were kept fixed at the values determined from the clean surface results (0.70 and 0.62 eV, respectively). Binding energies (in eV) are referred to the bulk As $3d_{5/2}$ binding energy. Column 1: hydrogen exposure in langmuirs. Column 2: average percent variation of the experimental points relative to the theoretical line shape, expressed as percent of the experimental peak amplitude. Columns 3 and 4: binding energy of the surface (E_s) and hydrogen-induced (E_h) 3*d* components. Columns 5, 6, 7, 8, 9 and 10: HWHM Γ and FWHM Δ (in eV) for the bulk (subscript *b*), surface (subscript *s*), and hydrogen-induced (subscript *h*) subcomponents. Column 11: integrated intensity of the surface-related As 3*d* doublet relative to the bulk As 3*d* emission. Column 12: intensity of the hydrogen-induced doublet relative to the surface doublet. Column 13: integrated intensity of the overall surface (surface + hydrogen-induced) 3*d* emission relative to the bulk 3*d* emission. In the fifth and sixth rows of the table we show line-shape parameters obtained keeping Lorentzian HWHM and Gaussian FWHM, respectively, fixed at the initial values.

		As 3*d* ($h\nu$=100 eV)										
	APV	E_s	E_h	Γ_b	Δ_b	Γ_s	Δ_s	Γ_h	Δ_h	I_s/I_b	I_h/I_s	$(I_s+I_h)/I_b$
clean	1.2%	−0.40		0.20	0.19	0.24	0.20			1.03	0.00	1.03
1×10^4 L	1.5%	−0.38	0.41	0.20	0.19	0.27	0.19	0.30	0.23	0.47	0.93	0.91
2×10^4 L	1.3%	−0.37	0.36	0.20	0.19	0.30	0.26	0.26	0.21	0.53	0.83	0.97
4×10^4 L	1.7%	−0.40	0.35	0.20	0.19	0.32	0.24	0.30	0.22	0.52	0.98	1.04
					Fixed Lorentzian widths							
4×10^4 L	2.1%	−0.39	0.36	0.20	0.20	0.24	0.24	0.24	0.22	0.58	0.84	1.07
					Fixed Gaussian widths							
4×10^4 L	1.7%	−0.37	0.35	0.20	0.19	0.32	0.20	0.30	0.20	0.45	1.02	0.90

TABLE IV. As 3*d* line-shape parameters obtained from a least-squares fitting procedure of the EDC's for the As 3*d* emission at $h\nu$=80 eV. The procedure and the symbols employed are identical to those used in Table III. Note the lower surface sensitivity of the results at $h\nu$=80 eV as compared to the results at $h\nu$=100 eV.

		As 3*d* ($h\nu$=80 eV)										
	APV	E_s	E_h	Γ_b	Δ_b	Γ_s	Δ_s	Γ_h	Δ_h	I_s/I_b	I_h/I_s	$(I_s+I_h)/I_b$
clean	1.7%	−0.37		0.19	0.14	0.23	0.14			0.68	0.00	0.68
1×10^4 L	1.3%	−0.36	0.31	0.20	0.14	0.29	0.14	0.23	0.14	0.39	0.58	0.62
2×10^4 L	1.4%	−0.37	0.35	0.20	0.14	0.29	0.14	0.30	0.14	0.43	0.78	0.78
4×10^4 L	1.3%	−0.37	0.36	0.20	0.14	0.29	0.14	0.30	0.14	0.40	0.84	0.73

Table IV line-shape parameters obtained through a fitting procedure in which the Lorentzian and Gaussian widths, respectively, of the surface and hydrogen-induced components (at an exposure of 4×10^4 L) were kept fixed at the initial values. Fixing the Gaussian widths has little effect on the AVP parameter, while fixing the Lorentzian widths yields a large increase in the parameter. In any case we emphasize that binding energies and relative intensities of the three As 3*d* components are largely unaffected by the detail of the fitting procedure employed (see, for example, the corresponding values in the three bottom-most rows of Table III).

B. Surface bonds

In general, during quantitative analysis of core photoemission data, one should not try to attach too much quantitative significance to results obtained from a fit of relatively broad experimental lines. Our approach has therefore been to start with the simplest possible physical assumption (the existence of three core components, i.e., bulk, surface, and hydrogen induced), obtain a least-squares best fit (1–2 % APV) with the minimum possible number of fitting parameters, and check for a systematic consistency of the fitting parameter values when varying the photon energy, and from cleave to cleave. The results of Tables I–IV satisfy all such criteria. The only limitation is in the hypothesis of the existence of only three core components, and some of the parameter variations in Tables I–IV may reflect the emergence of unresolved core contributions, as will be explained in the next section.

The results of Figs. 1 and 2 and Tables I–IV show that emission from the hydrogen-induced Ga 3*d* and As 3*d* doublets is primarily localized in the surface region. For example, in the Tables the hydrogen-induced Ga 3*d* and As 3*d* components exhibit the same intensity variation with photon energy observed for the Ga 3*d* and As 3*d* surface-related doublets. The maximum increase in intensity with exposure of the hydrogen-induced components (see Figs. 1 and 2) is observed between 0 and 1×10^4 L. This increase corresponds to a parallel decrease in the intensity of the As 3*d* surface (S) component. We associate the hydrogen-induced doublets with emission from Ga and As atoms directly bonded to hydrogen at the surface.

The binding-energy shift of the hydrogen-induced core component may provide information on the nature of the surface chemical bond. In Fig. 1 the hydrogen-induced Ga 3*d* levels appear initially 0.80 ± 0.05 eV below the bulk 3*d* component, and shift with increasing hydrogen exposure to higher binding energy. At 4×10^4 L the "chemical shift" is 0.98 ± 0.05 eV. The Ga 3*d* surface component remains, instead, at a binding energy of 0.27 ± 0.05 eV relative to the main line, confirming that this component is related to Ga surface atoms not directly interacting with hydrogen.

The hydrogen-induced As 3*d* component is observed 0.36 ± 0.05 eV below the bulk 3*d* component at all coverages explored. The As 3*d* surface component remains at a constant binding energy of 0.39 ± 0.05 eV relative to the main line, demonstrating that a portion of the As surface atoms are not bonded with hydrogen.

It would be tempting to interpret the observed chemical shifts in terms of hydrogen-induced charge transfer. The direction of the observed shifts would suggest charge transfer from Ga and As surface atoms to atomic hydrogen, in agreement with simple electronegativity arguments[31] (Pauling's electronegativities for H, As, and Ga are, respectively, 2.1, 2.0, and 1.6). Even the magnitude of the observed shifts follows the trend expected from the electronegativity difference (larger charge transfer for Ga-H than for As-H). However, several words of caution should be mentioned. In the present case no core level could be used to monitor the chemisorption-induced variation in electrostatic potential of the hydrogen atom. *Relative* chemical shifts should always be considered when possible to compensate for "parallel" shifts due to redistribution of the interstitial charge. More in general, even in those cases where it is possible to monitor core binding-energy shifts of both elements upon binary compound formation, the observed "chemical shifts" need not be related in an elementary way to the actual charge transfer.[29,32–34] Simple electronegativity arguments could not explain results for hydrogen chemisorption on InSb(110) surfaces,[15] when bonding of atomic hydrogen to In and Sb surface atoms was observed, the cation core levels exhibited a definite chemical shift, but only a broadening of the surface-related doublet was found for the anion cores.

In order to further clarify the adsorption mechanism of hydrogen on GaAs(110) surfaces we have examined the hydrogen-induced modification of the valence-band emission that accompany the core-level modification of Figs. 1 and 2. In Fig. 3(a) we show EDC's for the valence-band emission at $h\nu=60$ eV after subtraction of a smooth polynomial secondary background and normalization to the monochromator throughput. Curves labeled 1, 2, 3, and 4 correspond, respectively, to the clean GaAs(110) emission, and to exposure to 10^4, 2×10^4, and 3×10^4 L of hydrogen. The EDC's have been aligned to the valence-band maximum, estimated from a linear extrapolation of the leading valence-band edge in the clean spectrum, and from correction of band-bending variations as a function of hydrogen coverage.[35] Spectra at $h\nu=45$ eV showed similar results, and are not discussed here.

The spectra for the hydrogen-covered surface are all qualitatively similar, with emergence of dominant structure at about 5.5 and 8.5 eV. To emphasize the hydrogen-induced line-shape changes, we show in Fig. 3(b) difference curves obtained from the EDC's for the hydrogen-covered surface [curves 2, 3, and 4 in Fig. 3(a)] after subtraction of the clean surface spectrum [curve 1 in Fig. 3(a)]. All of the difference curves in Fig. 3(b) show significant reduction of the emission within 3 eV of the valence-band maximum. A similar phenomenon was observed in previous UPS studies[9] of the H-GaAs(110) system in the low-coverage regime, and associated with saturation of As-derived dangling bonds.[9] Here we also observe significant reduction in the valence-band emission in the 10–12 eV range as a result of hydrogen adsorption. A possible explanation is the removal of As-derived *s*-like surface states upon bonding with atomic hydrogen.[3]

Two new hydrogen-induced features appear in all of the difference curves in Fig. 3(b) at 5.5 and 8.5 eV. The position of the 5.5-eV feature is consistent with what is expected[3] for combinations of the hydrogen orbital with Ga-derived s-like states localized in the second atomic plane from the surface.[3] The second structure at 8.5 occurs instead within the heteropolar gap[3] and should be tentatively assigned to new hydrogen-induced localized states. The quenching of As-derived surface states and the emergence of new Ga-H hybrid features confirms that both Ga and As surface atoms are involved in the chemisorption process.

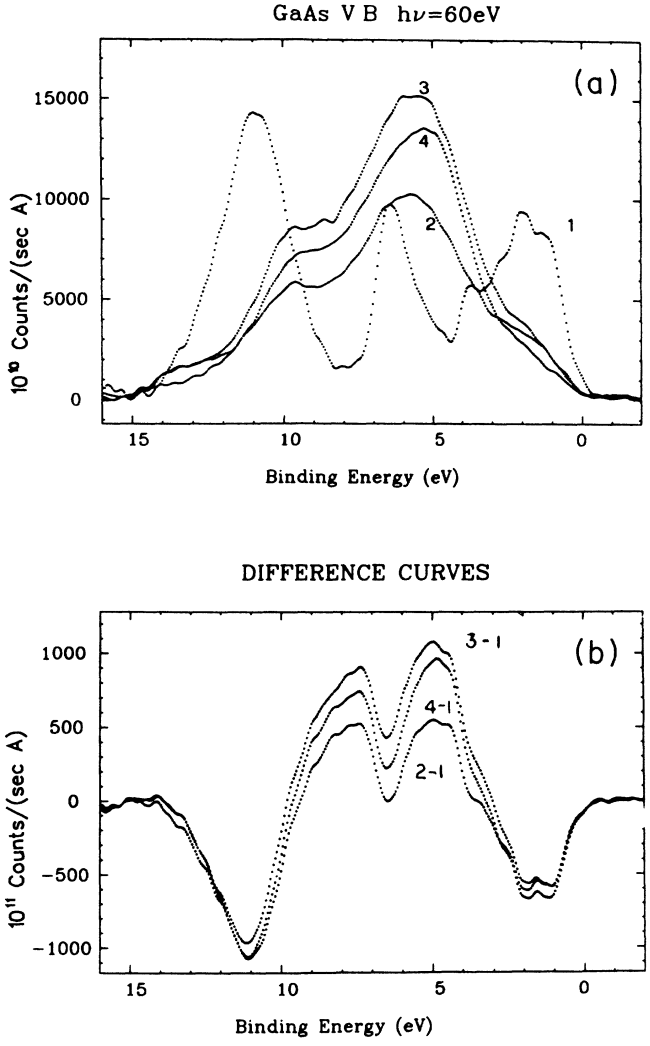

FIG. 3. (a) Valence-band EDC's at $h\nu=60$ eV for H-GaAs(110). All spectra have been aligned to the valence-band maximum that corresponds to the 0 of the binding-energy scale. The spectra are shown after background subtraction and normalization to monochromator throughput. Curves 1, 2, 3, and 4 correspond, respectively, to 0, 10, 20, and 40×10^3 L hydrogen exposure. (b) Difference curves obtained from EDC's 2, 3, and 4 in (a) after subtraction of the clean GaAs emission [EDC 1 in (a)]. The minima correspond to quenching of As-derived s-like surface states (10–12 eV) and As-derived dangling bonds (0–3 eV). The maxima to new Ga-H hybrid features (5.5 eV) and hydrogen-induced localized states in the heteropolar gap (8.5 eV).

C. Surface stoichiometry

In Fig. 4 we provide evidence that hydrogen chemisorption establishes a Ga-rich surface stoichiometry on GaAs(110). We show [Fig. 4(a)] EDC's for the As $3d$ and Ga $3d$ core emission as a function of hydrogen exposure in the $(4–12)\times10^4$ L range, at a constant photon energy of 100 eV. We used low-energy resolution (about 0.6–0.8 eV) to maximize the signal-to-noise ratio, and a single photon energy to simplify normalization procedures. In Fig. 4(b) we plot the corresponding ratio of the integrated emission intensities from the Ga $3d$ and As $3d$ core levels as a function of hydrogen exposure. The data exhibit little dispersion and indicate a linear increase in the

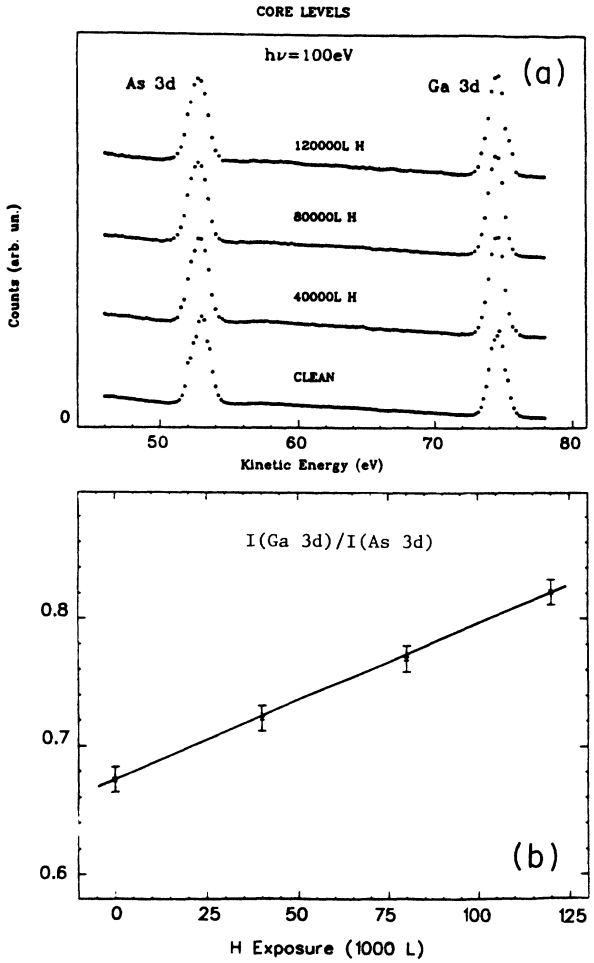

FIG. 4. (a) Low-resolution EDC's at $h\nu=100$ eV, for the As $3d$ and Ga $3d$ core emission from H-GaAs(110). (b) $I(\text{Ga } 3d)/I(\text{As } 3d)$ relative intensity as derived from the integrated emission of the core levels in (a). The linear increase in the intensity ratio reflects preferential As etching and Ga enrichment of the surface and near-surface regions.

$I(\mathrm{Ga})/I(\mathrm{As})$ ratio from 0.67 (clean surface) to 0.86 (12×10^4 L).

We can use the surface-sensitive decompositions of Figs. 1 and 2 to gauge the changes in surface stoichiometry that determine the intensity variation in Fig. 4(b). In the high-coverage regime we observe in Fig. 1 a twofold increase in the *overall* Ga $3d$ surface emission ($S+H$) relative to the bulk emission. Most of this increase is due to the hydrogen-induced $3d$ component (H), since the intensity of the "clean" surface component (S) remains relatively constant as compared to the bulk component with increasing hydrogen coverage. In the case of As in Fig. 2 and Table III, we observe a sharp decrease in the "clean" surface component (S), compensated by an increase in the hydrogen-induced component to yield a relatively constant *overall* As $3d$ ($S+H$) surface emission.

Together, the results of Figs. 1, 2, and 4 are consistent with an increase in the number of "surface-like" versus "bulk-like" atoms, and preferential Ga-enrichment of the surface with Ga atoms bonded to hydrogen. We propose that selective As etching through AsH_3 desorption,[6] roughening of the surface and formation of a disordered Ga-rich surface and/or near surface region can explain the results of Figs. 1–4. We emphasize that the increase in overall surface emission in Figs. 1 and 2 by itself does not necessarily imply surface roughening, since it could also be consistent with hydrogen penetrating in the semiconductor to affect more than one atomic layer. The increase in overall surface emission *together* with the change in surface stoichiometry (Fig. 4), however, argues for the proposed surface roughening as a result of preferential As etching. Roughening of the surface is also consistent with the results of LEED studies.[11]

A rough estimate of the maximum Ga enrichment observed can be made using the saturation values of the relative core intensities in Figs. 1 and 2 and Tables I and III to analyze the intensity variation in Fig. 4 in terms of overall surface ($S+H$) and bulk contributions. We estimate an increase in the overall [Ga]/[As] relative atomic concentration of 83% (including surface and hydrogen-induced components) in the surface layer at a hydrogen exposure of 12×10^4 L. The almost twofold increase in the [Ga]/[As] concentration in the surface layer is qualitatively consistent with the threefold increase in the $I(\mathrm{Ga})/I(\mathrm{As})$ Auger ratio reported in Ref. 11 at hydrogen exposures of 30×10^4 L. However, our results rule out the interpretation proposed by M'Hamedi *et al.*,[11] involving dissociation of the surface in metallic Ga droplets and chemisorbed AsH_3. The argument that As atoms in chemisorbed AsH_3 would not contribute to the MVV Auger signal because of orbital rearrangement,[11] has no bearing on our core photoemission results of Fig. 4. Furthermore, the high-resolution core deconvolutions of Fig. 1 and 2 shows no evidence of metallic or dissociated Ga, that would both correspond to characteristic low-binding-energy contributions to the Ga $3d$ core line shape.[36,37] We are therefore in the presence of a real, dramatic change in surface stoichiometry that is the result of preferential etching of As away from the surface.

The broadening of the Ga and (to a lesser extent) As surface- and hydrogen-related components in Tables I–IV is related to the establishment of disordered, Ga-rich surface and near-surface regions. In an ideal, perfect solid, Lorentzian and Gaussian widths have simple physical interpretations. The Gaussian width is related to the experimental energy resolution, and the Lorentzian width to the inverse of the final state lifetime. In disordered bulk solids, or alloys, local fluctuations in bonding angles and distances yield fluctuations in the local atomic coordination and charge distribution about the perfect solid values. If such fluctuations do not yield a net change in the *average* coordination and local charge distribution, one would expect symmetric broadening of the core line shape as a result. This would be observed as an increase in the Gaussian FWHM.[38] The Gaussian width parameter loses therefore its direct analytical interpretation and becomes, in part, a phenomenological parameter which accounts for initial state broadening.

The results of Tables I and III, however, indicate that the broadening is asymmetric, since it affects the Lorentzian width rather than the Gaussian width parameter. An increase in the Lorentzian width parameter due to disorder could reflect the emergence of unresolved high-binding-energy chemically shifted core components, and/or disorder-related effects. Asymmetric broadening of a core line can be expected, in general, if disorder yields a net increase or decrease in the average local atomic coordination. In the present case, because of the establishment of a rough, Ga-rich surface layer, one would expect for the Ga atoms at the surface a net decrease in the average number of nearest As neighbors, and an increase in the average Ga-H coordination. The observed asymmetric broadening of the Ga $3d$ *surface* component may therefore reflect emission from Ga surface atoms with reduced Ga-As coordination, which should exhibit larger surface shifts. The observed asymmetric broadening of the Ga $3d$ H-*induced* component may derive from unresolved H-induced components, reflecting increased Ga-H coordination at the surface.

For As, following the preferential surface-etching stage, asymmetric broadening of the *surface* component may be related to the increased emission from As atoms in the near-surface region, exhibiting core binding energies intermediate between the surface and bulk values. Asymmetric broadening of the H-*related* component may reflect, as in the Ga case, the emergence of unresolved $3d$ components corresponding to As atoms with increased As-H coordination. Since in the early stages of chemisorption hydrogen saturates As dangling bonds, while during etching As evolves from the surface in the form of AsH_3, the changes in the hydrogen-related As $3d$ emission are likely to reflect a monotonic increase in the As-H average coordination for the residual As atoms at the surface.

IV. CONCLUSIONS

Chemisorption of atomic hydrogen onto GaAs(110) surfaces in the high-coverage regime involves the forma-

tion of both Ga—H and As—H bonds at the surface. The corresponding chemical shifts of 0.80–0.98 eV and 0.30 eV of the Ga 3*d* and As 3*d* core levels, respectively, are consistent with the charge transfer expected from simple electronegativity arguments, but are in contrast with recent results for H-InSb(110). Large variations in core-level intensities as a function of hydrogen exposure are explained by hydrogen-induced etching of As through AsH_3 desorption at room temperature, surface roughening and the formation of a highly disordered Ga-rich surface region. At the highest coverages explored here (12×10^4 L) we estimate that surface reaction with hydrogen yields an increase of about 80% in the [Ga]/[As] relative concentration within the surface layer of the semiconductor.

ACKNOWLEDGMENTS

This work was supported in part by the Office of Naval Research under Grants No. 00014-84-K-0545 and 00014-89-J-1407, by the Center for Interfacial Engineering of the University of Minnesota, and by the Italian National Research Council. We thank R. E. Bringans and J. R. Chelikowsky for fruitful discussions, A. E. Jaworowski for providing us with a number of useful references, and K. Horn for comments, and for providing us with the data analysis program used in the early stage of this work. The Synchrotron Radiation Center of the University of Wisconsin–Madison is supported by the National Science Foundation, and we gratefully acknowledge the cheerful support of its staff.

---

*Present address: Laboratorio TASC dell'INFM, Padriciano 99, I-34012 Trieste, Italy.

†Present address: Istituto di Struttura della Materia del C.N.R., Via E. Fermi, I-00044 Frascati, Italy.

‡Present address: Xerox Corporation, Webster, NY 14580.

§Present address: IBM Corporation, Rochester, MN 55901.

[1]P. E. Gregory and W. E. Spicer, Surf. Sci. **54**, 794 (1976).

[2]R. Matz and H. Luth, Phys. Rev. Lett. **46**, 500 (1981).

[3]F. Manghi, C. M. Bertoni, C. Calandra, and E. Molinari, J. Vac. Sci. Technol. **21**, 371 (1982).

[4]R. D. Bringans and R. Z. Bachrach, Solid State Commun. **45**, 83 (1983); J. Vac. Sci. Technol. A **1**, 676 (1983); in *Proceedings of the 16th International Conference on the Physics of Semiconductors*, edited by M. Averous (North-Holland, New York, 1983), p. 854.

[5]F. Bartels, L. Surkamp, H. J. Clemens and W. Monch, J. Vac. Sci. Technol. B **1**, 756 (1983).

[6]W. Mokwa, D. Kohl, and G. Heiland, Phys. Rev. B **29**, 6709 (1984).

[7]F. Antonangeli, C. Calandra, E. Colavita, S. Nannarone, C. Rinaldi, and L. Sorba, Phys. Rev. B **29**, 8 (1984).

[8]P. K. Larsen and J. Polmann, Solid State Commun. **53**, 277 (1985).

[9]C. Astaldi, L. Sorba, C. Rinaldi, R. Mercuri, S. Nannarone, and C. Calandra, Surf. Sci. **162**, 39 (1985).

[10]J. A. Schaefer, Surf. Sci. **178**, 90 (1986).

[11]O. M'Hamedi, F. Proix, and C. Sebenne, Semicond. Sci. Technol. **2**, 418 (1987).

[12]M. Pedio, E. Colavita, and S. Nannarone (unpublished).

[13]S. Nannarone, C. Astaldi, L. Sorba, E. Colavita, and C. Calandra, J. Vac. Sci. Technol. A **5**, 619 (1987).

[14]J. Beyer, P. Kruger, A. Mazur, and J. Pollman, J. Vac. Sci. Technol. B **1**, 756 (1982).

[15]V. Hinkel, L. Sorba, and K. Horn, Surf. Sci. **194**, 597 (1988).

[16]P. Friedel, P. K. Larsen, S. Gourrier, J. P. Cabanie, and W. M. Gerits, J. Vac. Sci. Technol. B **2**, 675 (1984).

[17]M. Pinarbasi, N. Maley, M. J. Kushner, A. Myers, J. R. Abelson, and J. A. Thornton, J. Vac. Sci. Technol. A **7**, 1210 (1989); R. W. Bernstein and J. K. Grepstad, *ibid.* **7**, 581 (1989).

[18]A. E. Jaworowski, Mater. Sci. Forum (Switzerland) **38–41**, 1057 (1989); and Surf. Interface Anal. **14**, 27 (1989).

[19]EDC's for Cr, Pd, Mn, Al, and Au films gave quantitatively consistent values of Fermi cutoff position and width. The experimental energy resolution was estimated from the Fermi cutoff width. Such a value was consistent, within experimental uncertainty, with the energy resolution expected from the theoretical monochromator band pass and the theoretical energy resolution of the photoelectron spectrometer.

[20]See, for example, R. Ludeke, J. Vac. Sci. Technol. B **1**, 581 (1983); J. H. Weaver, M. Grioni, J. J. Joyce, and M. del Giudice, Phys. Rev. B **31**, 5290 (1985); W. Monch, Solid State Commun. **56**, 215 (1986), and references therein.

[21]D. E. Eastman and F. J. Himpsel, J. Vac. Sci. Technol. **20**, 609 (1982).

[22]D. E. Eastman, T. C. Chiang, P. Heimann, and F. J. Himpsel, Phys. Rev. Lett. **45**, 656 (1980).

[23]The surface sensitivity for the Ga 3*d* core levels increases in going from $h\nu=60$ to $h\nu=80$ eV. This is clearly seen in Tables I and II, where the Ga 3*d* surface-to-bulk ratio for the clean surface increases at $h\nu=80$ eV.

[24]R. Ludeke, T. C. Chiang, and D. E. Eastman, Physica B&C **117&118B**, 819 (1983).

[25]The experimental uncertainties quoted for the fitting parameters represent the distribution of parameter values encountered in analyzing EDC's at different photon energies (for the binding-energy parameters) or for different cleaves (for the width and intensity parameters).

[26]M. Taniguchi, S. Suga, M. Seki, S. Shin, K. L. T. Kobayashi, and H. Kanzaki, J. Phys. C **16**, 245 (1983).

[27]See, for example, K. C. Prince, G. Paolucci, V. Chab, M. Surman, and A. M. Bradshaw, Surf. Sci. Lett. **206**, L871 (1988), and references therein.

[28]J. D. Levine and P. O. Mark, Phys. Rev. **144**, 751 (1966).

[29]R. E. Watson and J. W. Davenport, Phys. Rev. B **27**, 6418 (1983); see also J. W. Davenport, R. E. Watson, M. L. Perlman, and T. K. Sham, Solid State Commun. **40**, 999 (1981).

[30]The surface sensitivity for the As 3*d* core levels increases in going from $h\nu=80$ eV to $h\nu=100$ eV. This is clearly seen in Tables III and IV where the As 3*d* surface-to-bulk ratio for the clean surface increases at $h\nu=100$ eV.

[31]L. Pauling, *The Nature of the Chemical Bond* (Cornell Univer-

sity Press, Ithaca, 1940).

[32]See, for example, R. E. Watson and M. L. Perlman, Struct. Bonding **24**, 82 (1975).

[33]See, for example, A. Franciosi, J. H. Weaver, and F. A. Schmidt, Phys. Rev. B **26**, 546 (1982), and references therein.

[34]We mention also that since atomic hydrogen bonds to Ga and As atoms at the surface, and since Davenport *et al.* (Ref. 29) and Monch (Ref. 20) demonstrated that the main contribution to the core surface shifts observed in III-V semiconductors derives from the Madelung term, one could argue that hydrogen-induced "chemical shifts" should be calculated relative to the binding energy of the surface component. We would then observe a chemical shift of (0.52–0.71)±0.04 eV for the Ga 3*d* line, and a parallel shift of 0.75±0.10 for the As 3*d* line. Such shifts would not scale with the magnitude of the electronegativity difference.

[35]Band bending was estimated from the parallel binding-energy variation of the Ga 3*d* and As 3*d* bulk core components.

[36]G. Margaritondo and A. Franciosi, Ann. Rev. Mater. Sci. **14**, 67 (1984).

[37]L. J. Brillson, Surf. Sci. Rep. **2**, 123 (1982).

[38]We mention that in random solids no band structure exists in the conventional sense, but it is possible to compute a Bloch spectral function which is strictly connected with the individual "bands" [see, for example, H. E. Ehrenreich and L. H. Schwartz, Solid State Phys. **31**, 149 (1976) and B. L. Gyorffy and G. M. Stocks, *Electrons in Disordered Metals and Metallic Surfaces,* edited by P. Phariseau [Plenum, New York, 1980]. The resulting "pseudoband structure" shows a broadening of several tenths of an eV of the empty one-electron states. Such disorder-induced broadening will affect any photoexcitation process, and can be expressed as the inverse of the lifetime of the one-electron final state of the photoexcitation event. The corresponding expected *Lorentzian* broadening [see for example A. Yariv, *Optical Electronics* (Holt, Rinehart and Winston, New York, 1985)] is clearly observed in the alloy optical spectra [see, for example, E. Colavita, A. Franciosi, R. Rosei, F. Sacchetti, E. S. Giuliano, R. Ruggeri, and D. W. Lynch, Phys. Rev. B **20**, 4864 (1979)].